Phenomenological Model for the Normal-State Angle-Resolved Photoemission Spectroscopy Line Shapes of High-Temperature Superconductors

Kazue Matsuyama and G.-H. Gweon*

Department of Physics, University of California, Santa Cruz, California 95064, USA

(Received 3 December 2012; revised manuscript received 17 July 2013; published 11 December 2013)

Providing a full theoretical description of the single-particle spectral function observed for high-temperature superconductors in the normal state is an important goal, yet unrealized. Here, we present a phenomenological model approaching towards this goal. The model results from implementing key phenomenological improvement in the so-called extremely correlated Fermi-liquid model. The model successfully describes the dichotomy of the spectral function as functions of momentum and energy and fits data for different materials ($Bi_2Sr_2CaCu_2O_{8+\delta}$ and $La_{2-x}Sr_xCuO_4$), with an identical set of intrinsic parameters. The current analysis goes well beyond the prevalent analysis of the spectral function as a function of momentum alone.

DOI: 10.1103/PhysRevLett.111.246401 PACS numbers: 71.10.Ay, 74.25.Jb, 74.72.Gh, 79.60.−i

In the sudden approximation theory [1] of the angle-resolved photoelectron spectroscopy (ARPES), photoelectron counts $I(\vec{k}, \omega)$ recorded as a function of momentum ($\vec{k}$) and energy (ω) [2] are given by

$$I(\vec{k}, \omega) = |M_{if}|^2 f(\omega) A(\vec{k}, \omega), \quad (1)$$

where M_{if} is the dipole matrix element for the photoexcitation, $f(\omega)$ is the Fermi-Dirac function, and $A(\vec{k}, \omega) = (1/\pi)\mathrm{Im}G(\vec{k}, \omega)$ is the single-particle spectral function, where G is the single-particle Green's function [3].

As the single-particle Green's function in the normal state is believed to contain vital information on the nature of excitations relevant to the high-temperature ("high-T_c") superconductivity, its characterization by ARPES has been a major line of research. Various approaches towards getting at this information have been attempted: a phenomenological approach based on a simple scaling behavior of the electron self-energy [5], an asymptotic solution to the Gutzwiller projected ground state of the t-J Hamiltonian [6], application of a non-Fermi-liquid theory [7] for low dimensions, and a newly proposed solution to the t-J Hamiltonian [4].

For an experimental "cut," i.e., an experimental data set taken along a line of $\vec{k}$ values, $I(\vec{k}, \omega)$ is a function defined on a two-dimensional domain. This multidimensionality makes analyzing $I(\vec{k}, \omega)$ a nontrivial task. While attempts [8] have been made to analyze the $I(\vec{k}, \omega)$ image [e.g., see Fig. 3(a)] as a whole, the current understanding of line shapes in terms of $A(\vec{k}, \omega)$ depends on the analysis of selected energy distribution curves [EDCs; the EDC is a function of ω, defined as $I(\vec{k} = \vec{k}_0, \omega)$] [4–6,9] or selected momentum distribution curves [MDCs; the MDC is a function of $\vec{k}$, defined as $I(\vec{k}, \omega = \omega_0)$, with $\vec{k}$ varying along a line] [9,10].

Currently, there is no consensus on a theoretical model that can suitably describe ARPES data of high-T_c materials. A model that can describe the normal-state data, both EDCs and MDCs, obtained in different experimental conditions and for different materials, with the same intrinsic parameters would be a good candidate. Here, we propose a new such phenomenological model.

The new model arises as the result of critically improving the so-called extremely correlated Fermi-liquid (ECFL) model [4], which was shown to be quite successful in describing EDCs. The new model now makes it possible to describe other key aspects of the data as well: MDC fits are excellent, and the values of $|M_{if}|^2$ behave reasonably. Moreover, it improves EDC fits. The result is a phenomenological model in which the apparent dichotomy between the EDCs and the MDCs [7,11] is described excellently by two independent aspects of a single theoretical concept, the caparison factor [4,12].

A phenomenological study of this kind seems to be helpful, also in light of the ongoing development of the ECFL theory [13,14]. The theoretical formalism of the ECFL initiated by Shastry [12,13] is quite involved, and, while a numerical solution [14] valid for hole doping $x \gtrsim 0.3$ is now available, more time seems necessary to extend these promising results to near-optimal doping. Thus, a phenomenological model based on the main feature of the theory, the caparison factor, may be of considerable value at this stage. In this theory [13], the caparison factor is an *ω-dependent adaptive spectral weight* that encodes two key pieces of physics: the Gutzwiller projection that reduces the spectral weight at high ω and the invariance of the Fermi surface volume at low ω.

In our previous work [4], it has been demonstrated that the normal-state EDCs for optimally doped cuprates for two different compounds, or for different experimental conditions (low photon energy or high photon energy), can be explained using an ECFL line shape model, all

with one set of intrinsic parameters. We will refer to that model as the "simplified ECFL (sECFL)" model [15], in relation to the fuller theory in development [13,14]. While the EDC analysis used there has strong merits [4,16], a natural subsequent question is whether MDCs can be described as well, along the same line of theory.

In the sECFL model [4], $G(\vec{k}, \omega)$ is given by

$$G(\vec{k}, \omega) = \frac{Q_n - \frac{n^2}{4}\frac{\Phi(\omega)}{\Delta_0}}{\omega - \varepsilon(\vec{k}) - \Phi(\omega)}, \quad (2)$$

where $Q_n = 1 - (n/2) = (1 + x)/2$ is the total spectral weight per $\vec{k}$ in the t-J model, and n (x) is the number of electrons (holes) per unit cell [17]. $\Phi(\omega)$ is an ordinary Fermi-liquid self-energy, determined by two intrinsic parameters $Z_{\rm FL}$ (quasiparticle weight) and ω_0 (cutoff energy scale) and one extrinsic parameter η (impurity scattering contribution to ImΦ). Δ_0 is an energy scale parameter, determined completely by n, $Z_{\rm FL}$, and ω_0, through the global particle sum rule. In the Supplemental Materials (SM) [18], a short summary of Ref. [4] is provided for readers' benefit.

The above Green's function can be rewritten as

$$G(\vec{k}, \omega) = \frac{Q_n}{\gamma_n} + \frac{\mathcal{C}_n(\vec{k}, \omega)}{\omega - \varepsilon(\vec{k}) - \Phi(\omega)}, \quad (3)$$

$$\mathcal{C}_n(\vec{k}, \omega) = Q_n\left(1 - \frac{\omega - \varepsilon(\vec{k})}{\gamma_n}\right), \quad (4)$$

where $\mathcal{C}_n(\vec{k}, \omega)$ is the "caparison factor" [4,12] and the energy scale Δ_0 is absorbed into $\gamma_n \equiv 4Q_n\Delta_0/n^2$. As all symbols in Eq. (3) other than $\Phi(\omega)$ are real,

$$A(\vec{k}, \omega) = \mathcal{C}_n(\vec{k}, \omega)A_{\rm FL}(\vec{k}, \omega), \quad (5)$$

where $A_{\rm FL}$ is the spectral function for the "auxiliary Fermi-liquid" Green's function [19] $A_{\rm FL} = (1/\pi)\text{Im}G_{\rm FL} = (1/\pi)\text{Im}[\omega - \varepsilon(\vec{k}) - \Phi(\omega)]^{-1}$.

The caparison function $\mathcal{C}_n$, summarized concisely in Eq. (4), played the central role in the sECFL model. In this work, we show how its role can be extended even further by a key phenomenological modification: inspired by data, we treat the ω dependence and the $\vec{k}$ dependence of $\mathcal{C}_n$ as separately adjustable. We shall refer to the modified model as the "phenomenological EFCL (pECFL)." We distinguish between the MD pECFL and the MI pECFL based on whether $\mathcal{C}_n$ remains momentum dependent (MD) or is made momentum independent (MI).

With this much introduction to our models, we shall first discuss line shape fits before discussing the models. As for free fit parameters controlling the line shape, all models have η and ω_0, like the sECFL [4] (cf. the SM, Sec. A). In addition, the group velocity v_{F0} of $\varepsilon(\vec{k})$ required small adjustment for different models to give correct peak positions (SM, Sec. B). Then, only for the MD pECFL, there are two more free fit parameters (see later).

Figure 1 shows ARPES line shape fits for the normal-state data for the optimally doped $Bi_2Sr_2CaCu_2O_{8+\delta}$ (Bi2212) sample, taken along the "nodal direction" $(0, 0) \rightarrow (\pi, \pi)$. Figure 1(a) shows fits essentially identical [20] with those of Ref. [4]. The fit quality of the MI pECFL is clearly the best, while that of the MD pECFL is noticeably poorer, despite more fit parameters.

Figure 2 shows ARPES line shape fits for MDCs of the same data set. Figure 2(a) shows clearly that the sECFL has difficulty fitting the data even at $\omega = 0$ (Fermi energy). Figure 2(b) shows a quite improved fit by the MD pECFL model. However, the MI pECFL fit shown in Fig. 2(c) is definitively the best.

That the MI pECFL model is able to describe EDCs and MDCs so accurately seems to confirm the basic ECFL idea [4]. In these fits, no extra component (e.g., extrinsic background intensity) was added to the theory that we described thus far [21]. All of the conclusions above also apply to the fits of the 91 K data [4], as shown in detail in the SM, Sec. C.

From the above work, it is clear that the MI pECFL model emerges as the best model for the Bi2212 data. This model is surprisingly simple: the $\varepsilon(\vec{k})$ term in Eq. (4) is simply dropped. The motivation for doing so is purely empirical: the MDCs of Bi2212 data are known to be quite symmetric and Lorentzian-like. The effect of this simple modification is surprisingly very good in many ways. MDC fits improve dramatically, as expected [Fig. 2(c)], but EDC fits improve also [Fig. 1(c)], especially for $\vec{k}$ far away from $\vec{k}_F$ [Fig. 3(b)]. Furthermore, the overall scale parameters

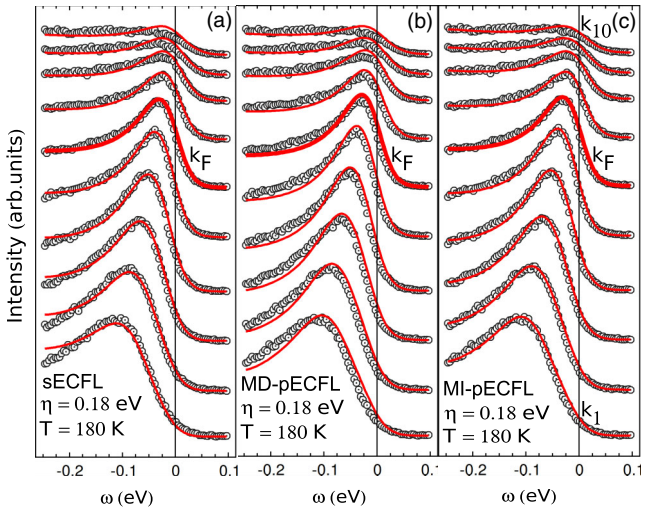

FIG. 1 (color online). Line shape fits of EDCs for Bi2212 ($x = 0.15$) using (a) sECFL, (b) MD pECFL, and (c) MI pECFL. Data and model parameters are identical with those in Ref. [4] ($Z_{\rm FL} = 0.33$, $\omega_0 = 0.5$ eV, $\Delta_0 = 0.12$ eV), except for slightly different values for η (0.17 → 0.18 eV) and $\varepsilon(\vec{k})$ (see the text).

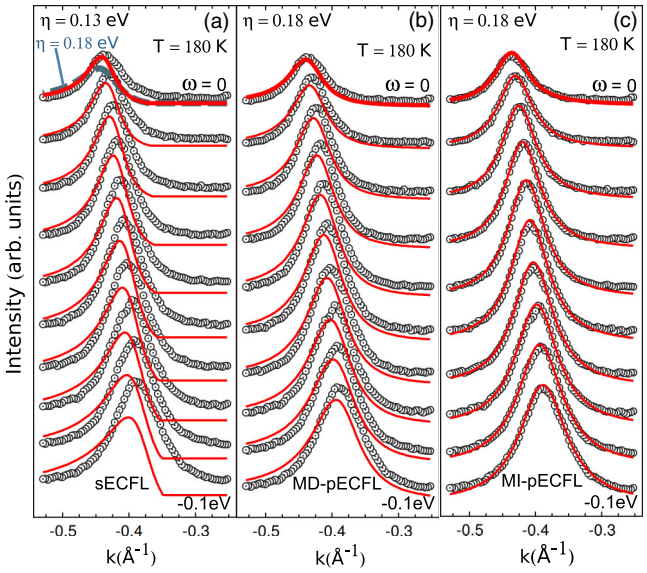

FIG. 2 (color online). Line shape fits of MDCs for Bi2212 ($x = 0.15$) using (a) sECFL, (b) MD pECFL, and (c) MI pECFL. Fit parameters are identical with those used for Fig. 1, except for the reduced η value (0.13 eV) for (a).

for MDC fits [Fig. 3(c)] and EDC fits [Fig. 3(d)] are now quite reasonable, as discussed in the caption. These facts lend an overwhelming support to the MI pECFL model.

The MI pECFL model accomplishes these feats *without* any additional fit parameter, in comparison to the sECFL model. Instead, the success arises crucially from the separate treatment of the ω dependence and the $\vec{k}$ dependence, or independence, of the caparison factor, important for describing EDCs and MDCs, respectively.

In contrast to the pECFL models, it is clear that the sECFL model cannot describe MDCs at all. Using identical fit parameters as for EDCs [see the dashed line marked "$\eta = 0.18$ eV" in Fig. 2(a)], we get very poor fit quality, which improves, dramatically but insufficiently, by relaxing the η parameter to 0.13 eV [Fig. 2(a)]. In this new light, the sECFL model, so successful in the previous work [4], must be viewed as getting only one of the two things correct—the ω dependence of the caparison factor, but not its $\vec{k}$ dependence—and its valid regime remains [4] confined to EDCs in the narrow range of $\vec{k}$ around $\vec{k}_F$ [Figs. 1(a) and 3(a); see also the SM, Sec. E].

How about the MD pECFL model? From our discussion up to this point, it does not seem worth much consideration. But, note that neither the sECFL nor the MI pECFL guarantees the fundamental requirement $\mathcal{C}_n(\vec{k}, \omega) \geq 0$ [Fig. 3(e)]. In the MD pECFL model, we take

$$\gamma_n = \gamma_{n0}\left[1 + \exp\left(\frac{\omega - \varepsilon(\vec{k}) - a_1\gamma_{n0}}{a_2\gamma_{n0}}\right)\right], \qquad (6)$$

where $\gamma_{n0} \equiv 4Q_n\Delta_0/n^2 = 0.38$ eV is the value of γ_n in the sECFL model. In the MD pECFL, $\mathcal{C}_n(\vec{k}, \omega) \geq 0$ *is*

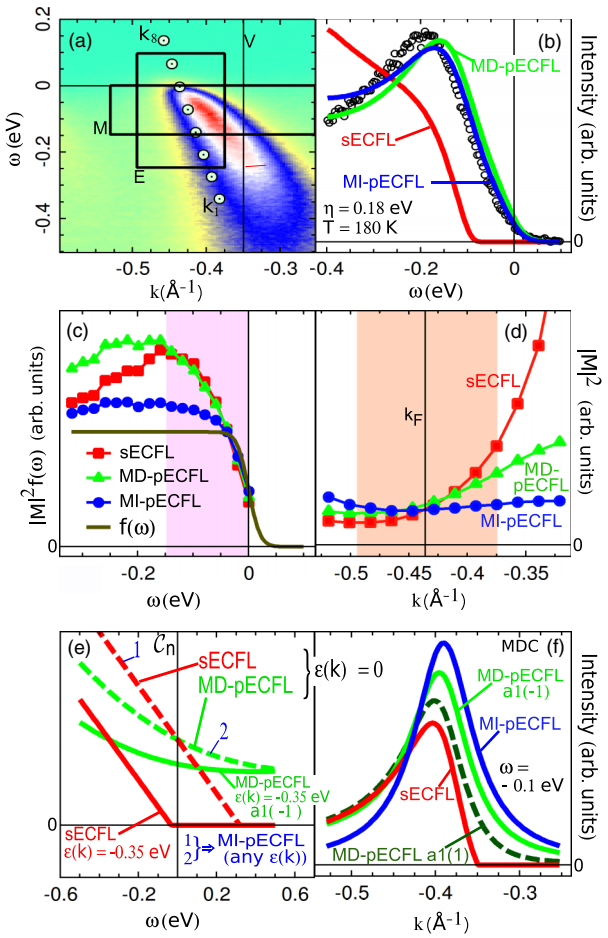

FIG. 3 (color online). (a) The ARPES data for Bi2212, fit in previous figures. Rectangle E (M) marks the range of data fit in Fig. 1 (Fig. 2). Circle symbols mark $\varepsilon(\vec{k})$ values used in the pECFL fits. The ARPES count increases from green, blue (half maximum), and white to red (maximum). (b) EDC and its fits, for the $\vec{k}$ value marked by the vertical line V in (a). (c), (d) The overall intensity scale parameters determined from (c) the MDC fit and (d) the EDC fit, which correspond to $|M|^2 f(\omega)$ and $|M|^2$, respectively, by Eq. (1). Shaded areas marks the fit ranges used in Figs. 1 and 2. As the energy dependence of $|M|^2$ is expected to be weak for this small range of ω, we expect the points shown in (c) to approximately follow $f(\omega)$ (solid line). The MI pECFL does this the best. We also expect points in (d) to show only a modest variation in this k range [8,31]. Here also, the MI pECFL performs the best; in contrast, the sECFL shows an unnatural steep increase. (e) $\mathcal{C}_n(\vec{k}, \omega)$ for various models used. For the MD pECFL, $a_1 = -1$ and $a_2 = 2$ are used throughout this Letter. For the sECFL, $\max(\mathcal{C}_n(\vec{k}, \omega), 0)$ is used [4]. (f) The evolution of the MDC asymmetry, controlled by a_1 within the MD pECFL ($a_2 = 2$). The MDC by the sECFL is the most asymmetric, while that by the MI pECFL is completely symmetric.

guaranteed for any $\vec{k}$ and ω values, if $a_1 \leq 1 + a_2(1 - \log a_2)$. Physically, a_1 and a_2 play the role of controlling the MDC asymmetry [Fig. 3(f)] and were determined as $a_2 = 2 \pm 1$ and $a_1 = -1 \pm 1$. See the SM, Sec. F, for details.

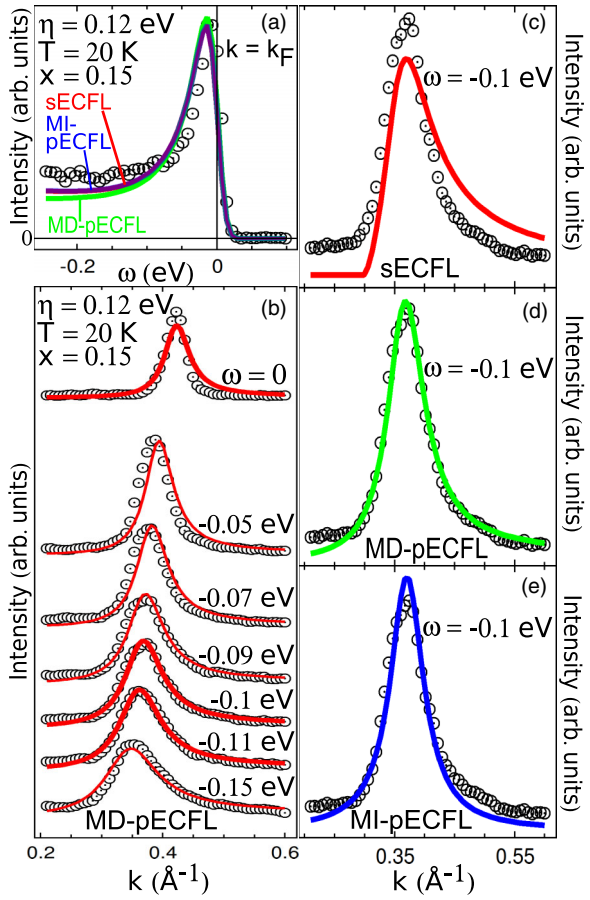

FIG. 4 (color online). Fits to the data of optimally doped ($n = 0.85$; $x = 0.15$) LSCO [22], taken along the nodal direction. (a) EDC fits at $k = k_F$. (b)–(e) MDCs for $-\omega \gtrsim 0.07$ eV are significantly asymmetric, described the best by the MD pECFL.

Accordingly, $\mathcal{C}_n$ for the MD pECFL stays clearly above zero and is smooth [Fig. 3(e)]. $\mathcal{C}_n$ for the MI pECFL is, by definition, that for the sECFL at $\varepsilon(\vec{k}) = 0$, as marked by label 1 in Fig. 3(e). However, we find that it can also be taken to be that for the MD pECFL at $\varepsilon(\vec{k}) = 0$, as indicated by label 2 in Fig. 3(e), since fit results are very comparable between these two choices.

For Bi2212, the MD pECFL is significantly better than the sECFL, but significantly worse than the MI pECFL, despite having two more fit parameters (cf. the SM, Sec. F).

However, the situation changes when we fit data of $La_{2-x}Sr_xCuO_4$ (LSCO) [22], showing strong MDC asymmetry [Figs. 4(b)–4(e)]. Here, identical fit parameter values as those for Bi2212 are used, except for $\eta = 0.12$ eV and v_{F0} (SM, Sec. B). Figure 4(a) shows an EDC fit, good by all models, just as for Bi2212. However, the MDC fit is a different matter. Notably, MDCs show significant asymmetry for $-\omega \gtrsim 0.07$ eV [Fig. 4(b)], and that asymmetry can be described properly only by the MD pECFL model, as illustrated clearly in fits shown in Figs. 4(b)–4(e), and as discussed further in Sec. D of the SM.

We see that the original sECFL model must be modified greatly (Bi2212) or somewhat (LSCO) to describe MDCs. We argue that these phenomenological modifications require physics beyond the t-J Hamiltonian, since the sECFL model is derived [12] from the t-J Hamiltonian, and another well-known model [16] based on the t-J Hamiltonian also implies too asymmetric MDCs. More specifically, the physics of the (next-nearest-neighbor hopping) t' term seems a good candidate: the well-known fact that $|t'/t|$ is significantly smaller for LSCO [23,24] goes well with our result that the MD pECFL model is more similar to the sECFL model. The t' term is correlated with the superconducting transition temperature [24], imparting importance to our current proposal. We recently found [25] that an anomalous ARPES feature is explained by the pECFL, but not the sECFL, and has similarity to a scanning tunneling spectroscopy feature correlated with superconductivity, adding more credence to our argument here. Last, the fact that the caparison factor for the infinite-dimensional ECFL becomes $\vec{k}$ independent [26,27] seems to go along with our result, within the crude analogy between adding a large t' term and increasing channels for t hopping. In sum, the variation between the sECFL and the pECFL, while consistent with the universal ω-dependent caparison factor of the ECFL theory, also points out the importance of the nonuniversal modification of the caparison factor within the ECFL theory.

In this Letter, we proposed a phenomenological ARPES line shape model, based on the ECFL theory [12,13]. The essential feature of our model remains the caparison factor [4,12,14], which is capable of describing both anomalous EDC line shapes [4,16], universal for high-T_c cuprates, and apparently more conventional MDC line shapes [9,10]. While our model is not the first to fit both EDCs and MDCs [9] of high-T_c cuprates, its demonstrated fidelity (including a qualitative description of $|M_{if}|^2$) and range of applicability are now unprecedented. Also unprecedented is the notable fact that our model requires a Dyson self-energy [28], whose form is drastically different from that assumed by the prevalent, but incomplete, MDC-only analysis [29,30]: to our knowledge, ours is the only $\vec{k}$-dependent [28] Dyson self-energy that has fit cuprate MDCs. Thus, extending the current analysis to wider ranges of momentum, doping, and temperature and studying its implications on other properties such as the resistivity [14] seems to make a great research topic for the immediate future.

We gratefully acknowledge B. S. Shastry and D. Hansen for stimulating discussions and feedback to the manuscript and G. D. Gu for Bi2212 samples used for the original data [4]. We thank T. Yoshida for sharing the digital version of the LSCO data. The work by G.-H. G. was supported partially by COR-FRG at UC Santa Cruz. Portions of this research were carried out at the SSRL, a Directorate of the SLAC National Accelerator

Laboratory and an Office of Science User Facility operated for the U.S. DOE Office of Science by Stanford University.

*Corresponding author.
gweon@ucsc.edu

[1] L. Hedin and S. Lundqvist, in *Solid State Physics*, edited by F. Seitz, D. Turnbull, and H. Ehrenreich (Academic, New York, 1969), Vol. 23, p. 1.
[2] Throughout this Letter, $\hbar = 1$ by convention.
[3] We use the advanced Green's function as in Ref. [4].
[4] G.-H. Gweon, B. S. Shastry, and G. D. Gu, Phys. Rev. Lett. **107**, 056404 (2011).
[5] C. M. Varma, P. B. Littlewood, S. Schmitt-Rink, E. Abrahams, and A. E. Ruckenstein, Phys. Rev. Lett. **63**, 1996 (1989).
[6] P. W. Anderson, Phys. Rev. B **78**, 174505 (2008).
[7] D. Orgad, S. A. Kivelson, E. W. Carlson, V. J. Emery, X. J. Zhou, and Z. X. Shen, Phys. Rev. Lett. **86**, 4362 (2001).
[8] W. Meevasana, F. Baumberger, K. Tanaka, F. Schmitt, W. R. Dunkel, D. H. Lu, S.-K. Mo, H. Eisaki, and Z.-X. Shen, Phys. Rev. B **77**, 104506 (2008).
[9] A. Kaminski, H. M. Fretwell, M. R. Norman, M. Randeria, S. Rosenkranz, U. Chatterjee, J. C. Campuzano, J. Mesot, T. Sato, T. Takahashi, T. Terashima, M. Takano, K. Kadowaki, Z. Z. Li, and H. Raffy, Phys. Rev. B **71**, 014517 (2005).
[10] T. Valla, A. V. Fedorov, P. D. Johnson, B. O. Wells, S. L. Hulbert, Q. Li, G. D. Gu, and N. Koshizuka, Science **285**, 2110 (1999).
[11] G.-H. Gweon, J. W. Allen, and J. D. Denlinger, Phys. Rev. B **68**, 195117 (2003).
[12] B. S. Shastry, Phys. Rev. Lett. **107**, 056403 (2011).
[13] B. S. Shastry, Phys. Rev. B **87**, 125124 (2013).
[14] D. Hansen and B. S. Shastry, arXiv:1211.0594.
[15] B. S. Shastry, Phys. Rev. Lett. **108**, 029702 (2012).
[16] P. A. Casey, J. D. Koralek, N. C. Plumb, D. S. Dessau, and P. W. Anderson, Nat. Phys. **4**, 210 (2008).
[17] We now use the symbol $\varepsilon(\vec{k})$, instead of $\xi(\vec{k})$ (Ref. [4]), for the one electron energy.
[18] See Supplemental Material at http://link.aps.org/supplemental/10.1103/PhysRevLett.111.246401 for a brief summary of key results of Ref. [4], technical details of line shape fits, and the detailed discussion of the line shape fits of the 91 K data.
[19] As in Ref. [4], the subscript "FL" means the auxiliary Fermi liquid throughout this Letter.
[20] The slight difference is due to a slight change of η ($0.17 \rightarrow 0.18$ eV), noted in the caption of Fig. 1.
[21] A small "elastic background line shape" (0.5 times the raw line shape for $k \gg k_F$) had been subtracted prior to the fit, as explained in Ref. [4].
[22] T. Yoshida, X. J. Zhou, D. H. Lu, S. Komiya, Y. Ando, H. Eisaki, T. Kakeshita, S. Uchida, Z. Hussain, Z.-X. Shen, and A. Fujimori, J. Phys. Condens. Matter **19**, 125209 (2007).
[23] R. S. Markiewicz, S. Sahrakorpi, M. Lindroos, H. Lin, and A. Bansil, Phys. Rev. B **72**, 054519 (2005).
[24] E. Pavarini, I. Dasgupta, T. Saha-Dasgupta, O. Jepsen, and O. K. Andersen, Phys. Rev. Lett. **87**, 047003 (2001).
[25] G.-H. Gweon, G.-D. Gu, J. Schneeloch, R. D. Zhong, and T. S. Liu, arXiv:1310.4668.
[26] R. Zitko, D. Hansen, E. Perepelitsky, J. Mravlje, A. Georges, and B. S. Shastry, arXiv:1309.5284.
[27] E. Perepelitsky and B. S. Shastry, arXiv:1309.5373.
[28] B. S. Shastry, Phys. Rev. B **84**, 165112 (2011).
[29] J. Kokalj and R. H. McKenzie, Phys. Rev. Lett. **107**, 147001 (2011).
[30] J. Chang, M. Shi, S. Pailhs, M. Månsson, T. Claesson, O. Tjernberg, A. Bendounan, Y. Sassa, L. Patthey, N. Momono, M. Oda, M. Ido, S. Guerrero, C. Mudry, and J. Mesot, Phys. Rev. B **78**, 205103 (2008).
[31] A. Bansil and M. Lindroos, J. Phys. Chem. Solids **59**, 1879 (1998).